Συμπεριφορά Ινοπλισμένων Σκυροδεμάτων σε Πειράματα Άμεσης Διάτμησης (Push-off)

Behavior of Fiber Reinforced Composites Under Direct Shear (Push-off tests)

Αντρούλα ΓΕΩΡΓΙΟΥ[1], Σταυρούλα ΠΑΝΤΑΖΟΠΟΥΛΟΥ[2]

ΠΕΡΙΛΗΨΗ : Το άρθρο μελετά την μηχανική συμπεριφορά τσιμεντούχων ινοπλισμένων σκυροδεμάτων υπό άμεση διάτμηση. Το σκυρόδεμα περιέχει κατά 60% αντικατάσταση του τσιμέντου με ιπτάμενη τέφρα και 2% (επί του όγκου) συνθετικές ίνες κατανεμημένες στη μάζα του (ίνες Πολυβυνιλικής Αλκοόλης, PVA), και λεπτόκοκκα αδρανή μόνον. Αυτή η κατηγορία ινοπλισμένων τσιμεντοειδών παρουσιάζουν πλαστιμότητα στον εφελκυσμό που επιτυγχάνεται με την διάνοιξη πολλαπλών λεπτών ρωγμών και καθυστέρηση της σταθεροποίησης της ρηγμάτωσης (σε αντίθεση με την συγκέντρωση αστοχίας σε μία μόνο ρωγμή). Μια κύρια παράμετρος συμπεριφοράς που αφορά τον δομικό σχεδιασμό κατασκευών είναι η διατμητική αντοχή του νέου ινοπλισμένου σκυροδέματος. Η διατμητική αντοχή του ινοπλισμένου σκυροδέματος μελετήθηκε με την χρήση του πειράματος καθαρής διάτμησης (Push-off). Η διατμητική αντοχή στη συνέχεια συγκρίνεται με την αντοχή των υλικών σε άμεσο εφελκυσμό και διάρρηξη.

ABSTRACT : In this paper the mechanical behavior of Advanced Cement-Based materials under direct shear is studied. The composite material considered contains 60% replacement of cement with fly ash and 2% (volume ratio) of short discontinuous synthetic fibers (mass reinforcement, comprising PVA - Polyvinyl Alcohol fibers). This class of cementitious materials exhibits ductility under tension with the formation of multiple fine cracks and significant delay of crack stabilization (i.e., localization of cracking at a single location). One of the behavioral parameters that concern structural design is the shear strength of this new type of fiber

---

[1] Research Assistant, Department of civil and Environmental Engineering, University of Cyprus, email: ageorg44@ucy.ac.cy

[2] Professor, Department of Civil Engineering, Lassonde Faculty of Engineering, York University, Toronto, Canada, email: pantazo@yorku.ca

reinforced composites. This aspect was studied in the present work with the use of Push-off tests. The shear strength is then compared to the materials' tensile and splitting strength values.

INTRODUCTION

Sustainable design of structures leads to the need to reduce the materials being extracted from the earth (aggregates, cement) and replace them with recycled aggregates or industrial byproducts, such as high amounts of fly ash (>50%) but also combine the use of fibers in order to increase the durability of structures and their expected life time (Georgiou and Pantazopoulou 2016a). Fly ash in high amounts acts both as a pozzolan and as filler. Research in the past few decades is increasingly oriented to new types of cementitious composites with improved tensile properties by the introduction of fibers within the cementitious matrix. In the case of synthetic fibers a new type has lately been developed, called Polyvinyl-Alcohol (PVA) fibers, that due to their hydrophilic surface, they create strong chemical bonds with the surrounding matrix – see for example, Li et al. 2003; Georgiou and Pantazopoulou 2016b. In the latter research it was found that the strength of the interfacial bonds ought to be moderated – through proper surfactants on the fiber surface, in order to eliminate the tendency for crack localization with increasing age, and in order to ensure fine distributed cracking in FRCC (fiber reinforced cementitious composite with synthetic fibers, Naaman and Reinhardt 2006).

The emerging Strain Hardening Fiber Reinforced Cementitious Composites (SHFRCC) is a special category of Strain Resilient FRCCs, which not only present toughness to large tensile deformation, but also strain hardening properties. The entire class of these materials have a matrix that lacks any coarse aggregates, containing only fine high quality sand with maximum particle size less than 300μm. Additionally for improving the sustainability of these composites the matrix has great amounts of cement replacement to fly ash, even in the order of 60%. This special class of cement-based composites have shown enhanced flexural performance whereas their tensile strain hardening behavior mitigates susceptibility of shear resistance to cracking. Tests conducted on structural members reveal that this beneficial effect is inherited to the overall structural performance (Georgiou and Pantazopoulou 2017a; Toshiyuki et al. 2013). Elimination of coarse aggregate means that there is no aggregate interlock – which, in conventional concrete is considered an essential source of post-cracking shear strength. Instead, in FRCC the postcracking shear strength is – to a large extent – owing to the use of the short fibers. Other mechanisms such as dowel action and compressive strength of cracked concrete also prevail in the FRCC members, however, there is a need to better understand these strength components and to quantify the shear resistance of steel reinforced FRCC members for the benefit of practical design.

Based on past tests on FRC it is generally known that fibers generally improve shear strength and ductility of concrete and that they may partially replace the use of

stirrups. To extrapolate these concepts to SHFRCC, direct shear tests conducted on push-off specimens are used in the present study to explore and explain the role of the fibers in the mechanics of shear of FRCC members.

EXPERIMENTAL PROGRAM

Test Specimens

Tests were carried out on a series of specimens to determine the uniaxial material stress-strain curves in direct and indirect tension, in direct compression, as well as the shear behavior of SHFRCC. Uniaxial compression tests were performed on cylinder specimens 100 mm in diameter and 200 mm in height, having an aspect ratio of 2 in order to eliminate the local end effects, under displacement control, at a loading rate of 1.5 μm/s.

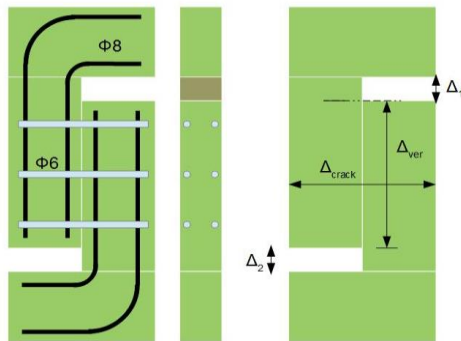**Table 1.** Specimen Denomination

Identification	Mix design	Stirrups
HVFA	HVFA	-
HVFA-S	HVFA	6Φ6
SHCC	SHCC	-
SHCC-S	SHCC	6Φ6

Figure 1. (a) Push-off specimen and (b) definition of deformation for graphical representation

For the determination of uniaxial tensile strength both direct tension (dog-bone type) tests and split cylinder tests were conducted. Direct tension tests were performed at a displacement control rate of 2.5 μm/sec with a gauge length of 100 mm. Deformations were recorded with two LVDTs mounted on opposite sides of the specimens. The split cylinders had a diameter of 100mm and a height of 100 mm. The splitting tests were under displacement control at a displacement rate of 0.5 mm/min.

Direct shear was studied with push-off tests on properly designed specimens (Fig. 1); these had dimensions of 250x500x100 mm, with two antisymmetric lateral notches to define a shear plane area of $100x200=20000$ mm^2 (Valle and Buyukozturk 1993, Buyukozturk et al. 1990). Two parameters were investigated:

a) the mix design – i.e., with or without fibers: a.1) HVFA the mix with a high volume fly ash as cement replacement and a.2) SHCC the same mix with the addition of PVA fibers

and b) the presence of steel stirrups crossing the shear plane. The specimens with stirrups had the configuration shown in Fig. 1 (a). Three identical specimens were tested for each type of test and mix design. The specimen's classifications and name

are outlined in Table 1. Specimens were tested at the age of 100 days, in order to acquire the long term mechanical properties of the composites, since the presence of fly ash, as well as the coating of the fibers, change the interfacial bond properties between the fibers and the matrix through time. Therefore the multiple cracking phenomenon is seen at its most unfavorable state when specimens tested are older than 28 days gradually leading to a reduced strain capacity (Georgiou et al. 2014). For the push-off specimens LVDTs were used to measure displacements at various positions. Note that the horizontal relative displacement of the vertical specimen boundaries is actually the crack width of the shear plane. The speed was 15 μm/sec.

Materials

The mix designs used for the plain mix with high volume of fly ash (HVFA) and the same mix with the fibers (SHFRCC) are listed in Table 2. Portland Composite Cement 42.5 R and silica sand (>95% Si) with a maximum grain size of 300 μm were used. Type F imported fly ash was used as cement replacement. PVA fibers (12mm long, 39 μm diameter) were used at 2% volume fraction, with 1300 kg/m^3 density, nominal tensile strength of 1600 MPa and 40 GPa Young's Modulus. The fibers were coated with a pertinent surfactant at a weight ratio of 6.6% (of the fibers used). Past studies have shown that coating the PVA fibers increases their dispersion whereas the final ductility of composites is controlled by the bond properties at the fiber - matrix interface (Georgiou et al. 2014). Steel reinforcement had a yield strength of 300 MPa for the stirrups with 200 GPa modulus of elasticity. Smooth bars (6 mm diameter) were used for stirrup reinforcement (hook-anchored into the member core).

Table 2: Mixture proportions (*per weight, $^+$ per volume)

MIX	Cement*	Fly Ash*	Sand*	Water*	Superplasticizer*	Fibers$^+$	Coating*
HVFA	1.00	1.20	0.80	0.55	0.012		
SHCC	1.00	1.20	0.80	0.60	0.017	2%	6.6%

RESULTS AND DISCUSSION

Material Properties in Tension and Compression

In the case of the HVFA mix (i.e., plain matrix) the three samples that were cast for uniaxial tension, cracked during their de-molding. The SHFRCC mix on the other hand demonstrated strain hardening response in uniaxial tension: during the phase of multiple crack formation, stress capacity of the cross section increased. Details of the experimental setup for the uniaxial tensile test are given elsewhere (Georgiou and Pantazopoulou 2016a). Past a notional yield point multiple cracks formed whereas fibers were bridging the cracks transferring load. Formation of cracks saturated the full length till the occurrence of crack localization and failure The fracture energy G_f

defined as the area under the stress-crack opening curve in the strain softening branch past the ultimate stress was estimated as G_f=1065 N/m for the SHCC - a value much greater than the expected one for ordinary strength cement mortars and concretes which is in the order of 50 N/m and 130 N/m respectively (Archontas and Pantazopoulou 2015). To acquire the tensile strength of the HVFA composite splitting test was employed based on the ASTM Standard specifications (ASTM C496 2006) as $f_{split}=2P\ /(\pi l \cdot d)$. The average Load P at failure of the three HVFA specimens was P=30 kN, (the average modulus of rupture was $f_{t,r}$=1.9 MPa whereas the splitting tensile strength of the SHFRCC mix was f_{split}=6.4 MPa).
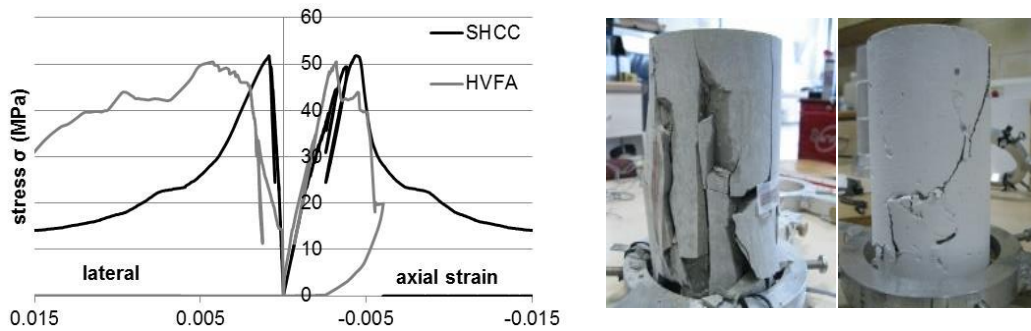

Figure 2. (a) Stress - axial/lateral strain diagrams under compression of HVFA and SHCC mixes, (b) failure cracks for HVFA and (c) failure cracks for SHCC

Figure 2 (a) compares the stress - axial strain - lateral strain diagrams obtained from compression tests conducted on one of the specimens with the use of fibers (SHFRCC) and of one of the tested specimens of the same matrix without the fibers (HVFA). The average compressive strength of the latter reaches 50.4MPa, but with the addition of fibers the average strength decreases to 49.0MPa. An increase by more than 30% occurred in the axial deformation that corresponds to peak load as compared to the corresponding values for plain mixes in the case of the matrix with the fibers (average strain at peak stress from -0.0032 for the HVFA to -0.00459 for the SHFRCC), as well as a stable descending branch. Based on the uniaxial compression experimental results of fiber reinforced cementitious composites as shown in Fig. 2 multiple cracking is evident all around the specimen. No evidence of deterioration or collapse is exhibited even after a 60% drop of the postpeak capacity under compression. In the case of the plain matrix deterioration is exhibited along with sudden collapse of the specimen if no confinement is used. The use of fibers changes the mode of failure. Lateral deformation is responsible for the rate of descend of the post peak branch. Fibers mobilized in the lateral direction can bridge cracks, transferring load and limiting lateral expansion of the cylinder under compression (Georgiou and Pantazopoulou 2017b). This is evidenced by the

restricted growth of post-peak lateral strain of the mix with fibers as compared to the plain concrete specimens. The stress-strain curves suggest that past the peak load, concrete with fibers behaves as if internally confined. The intensity of confinement is directly related to the materials' strength under splitting as found in previous research (Georgiou and Pantazopoulou 2017b).

Push-off test results and discussion

Failure modes of all tested specimens are depicted in Figure 3(c). Specimens HVFA without steel stirrups failed in a brittle mode as soon as the shear plane reached peak shear strength. The specimen with steel reinforcement (HVFA-S) started to delaminate rapidly with spalling of the cover after cracking at the shear plane. Spalling reached half of the width of the specimen (125 mm) and deformation of the steel reinforcement was visible over the entire deteriorated zone. In the case of the fiber reinforced mix without stirrups multiple cracking was observed prior to crack localization and failure of the sample. The cracks formed inclined to the vertical shear plane, with evidence of compression crushing at the edges of the shear plane. Failure of the fibers crossing the cracked planes was mixed between rupture and pull-out. The width of the process zone (where cracks occurred) was approximately 40 mm but in no case was the composite laterally delaminating. The same type of crack development was evident in the fiber reinforced matrix with stirrups crossing the shear plane. In these specimens though, the inclination of the cracks was greater than the inclination developed in the specimens without the steel reinforcement. Small dislocation of the cracks occurred at the locations where the steel stirrups were crossing the cracks. The width of the process zone was in the order of 60 mm, without spalling of the fiber cementitious matrix. The tests in this case were terminated at the point where shear deformation was no longer possible – the vertical dislocation was enough to close the lateral notches. Transverse reinforcement dowelled by 25 mm, a deformation that took place within the 60 mm process zone. The inclination angles of the cracks for the various specimens is HVFA with $\theta=90^o$, HVFA-S with $\theta=80.54^o$, SHCC with $\theta=66.37^o$ and SHCC-S $\theta=83.38^o$.

The experimental curves between machine load and various measures of deformation of the push-off specimens (defined in Fig. 1b) are plotted in the diagrams of Figure 3 (a). The crack opening Δ_{crack} for the specimen with stirrups and no fibers (HVFA-S) shows a near to zero lateral expansion up to the maximum load. At maximum load the crack is created and after that, deformation accounts for the crack opening width. The small lateral expansion that develops prior to the maximum load is attributed to elastic deformations. In the beginning of the descending branch the load capacity diminishes from maximum linearly with the increasing crack width, manifesting the loss of concrete contribution to the shear resistance. The remaining strength that continues to be constant, for greater deformations, is the contribution of the steel reinforcement to the shear capacity. The

vertical deformation Δ_{vert} of the shear plane (between the crack faces) is in good agreement with the upper and lower recess deformations, Δ_1 and Δ_2 respectively (Fig. 1b). Here the slope of the ascending branch shows that shear deformation increases shear resistance prior to crack localization, with deformations of the shear plane up to 2 mm (length of shear plane is 200 mm). After a crack is formed, shear capacity diminishes down to the contribution of the steel reinforcement crossing the shear plane.
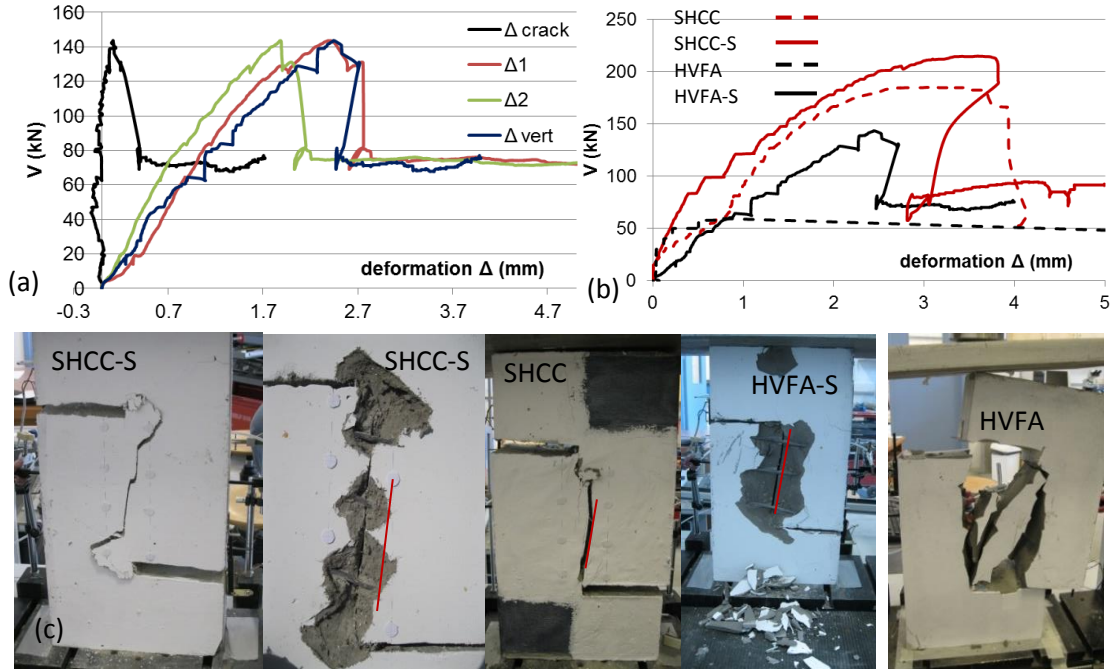

Figure 3. a) Push-off tests Load-Deformation curves for specimen HVFA-S-1 (with stirrups and no fibers), b) Push-off Load versus vertical deformation (Δ_{vert}) for different specimens and c) Push-off crack patterns for all specimens

In Figure 3 (b) the diagrams of shear load versus normalized crack opening of one of the three specimens from each series are displayed for the push-off tests. The beam with the HVFA mix and without steel reinforcement showed abrupt failure at an average load of 54.5 kN. After the peak load that was accompanied by a strong noise the specimen was split in two pieces. Average shear stress attained by these specimens was in the order of 2.5 MPa, calculated as the total applied load divided by the cross section area under shear. The addition of steel reinforcement (6 bars of 6 mm diameter) to the specimens without fibers increases the shear capacity in the order of 152.4 kN (7.3 MPa), while the addition of fibers only of 2% by volume

increases the shear capacity to 186.8 kN (9.17 MPa), triple of that of the plain mix. Also the addition of fibers increases the shear deformation on the vertical axis of symmetry of the specimen, and while the plain mix breaks at a shear deformation of $\gamma=0.5/200=0.25\%$, the mix with the fibers reaches a deformation of $3.5/200=1.75\%$. Shear stress seems to increase in the specimens with the fiber reinforced mixes, even though compressive strength of the SHFRCC mix is almost the same with that of the plain mix. This implies that shear strength is related mainly with the tensile stress-strain relationship of the mixes and not with the compressive strength. Stiffness of the specimens is greater in the case of the samples with stirrups, manifesting that steel reinforcement plays an important role in resisting shear even prior to crack initiation. In the case of the SHFRCC mix without the steel stirrups, cracking initiates at shear stresses close to 1/3 of the maximum shear stress of the samples and past that point stresses are transferred across the crack through the fibers, thereby developing a type of tension stiffening. At ultimate load of the plain SHFRCC fibers start to rupture and the specimen collapses. All samples containing steel reinforcement after the ultimate load, exhibited a load drop down to an average shear stress of 4 MPa, where only stirrups continue to resist shear, and while this value remained constant in the case of the mix without the fibers, there was an increase in resistance in the case of the fiber reinforced matrix, relating bending resistance of the stirrups to the tensile characteristics of the surrounding matrix.

Test results from all mixes are summarized in Table 3. Compressive strength is an average of three samples, while all results regarding push-off are thoroughly given for each specimen. Average maximum shear stress τ_{max} is obtained, by dividing the maximum load applied from the machine, by the area of the shear plane. Shear stresses developed in the HVFA specimens without steel reinforcement are equivalent to the direct tensile strength of the composite, while the introduction of steel reinforcement almost triples the shear capacity for the material without fibers. The introduction of fibers in the cementitious matrix triples the shear capacity of the cross section (from 55 MPa for HVFA to 186 MPa for SHCC). The use of PVA fibers results to shear a strength in the order of 9.16 MPa, a value that is much greater than the tensile strength of the fiber reinforced composite. Adding fibers of 2% by volume results in a higher shear strength than those cases using only steel reinforcement. Adding stirrups in the SHFRCC specimens is not as effective – increasing the shear capacity by only 10% over the unreinforced SHFRCC case.

Table 3. Push-off test results for all mixes

Specimen	f_c'	f_t	Max. Load	τ_{max}	$\tau_{max}/\sqrt{f_c'}$	τ_{max}/f_t
HVFA	50.37	1.91	54.49	2.49	0.35	1.31
HVFA-S	50.37	1.91	152.41	7.29	1.03	3.82
SHCC	48.98	2.75	186.82	9.17	1.31	3.33
SHCC-S	48.98	2.75	212.07	10.25	1.47	3.73

Shear strength and dowel action mechanics

The average load capacity of the 100x200 mm cross section for the HVFA composite without steel reinforcement was 49.87 kN. The shear strength was τ_{ave} =2.5 MPa based on the push-off test, while tensile strength based on the splitting test was 2 MPa. The increase of 0.5 MPa in the case of the push-off test can be attributed to some variation of the shear stress distribution over the shear plane and to some compressive stresses that developed close to the edges of the plane. When steel reinforcement was crossing the critical cross section (HVFA-S) maximum load was increased to 152 kN but after the crack opened such as the two sides had no contact between them, the load dropped suddenly to an average of 75.74 kN, representing the dowel action of the stirrups.

Thus, the SHFRCC composite's contribution to shear is taken as the strength difference from peak load after subtracting the dowel action which was measured in the reinforced specimens, equal to 70.13 kN (τ_{ave} = 3.79 MPa). Due to the inclination of the shear cracks in this case (main crack of HVFA-S is θ=80.54°) and the simultaneous action of the reinforcement that induces confinement on the composite, a biaxial stress state develops (where shear strength necessarily exceeds the tensile strength of the composite.
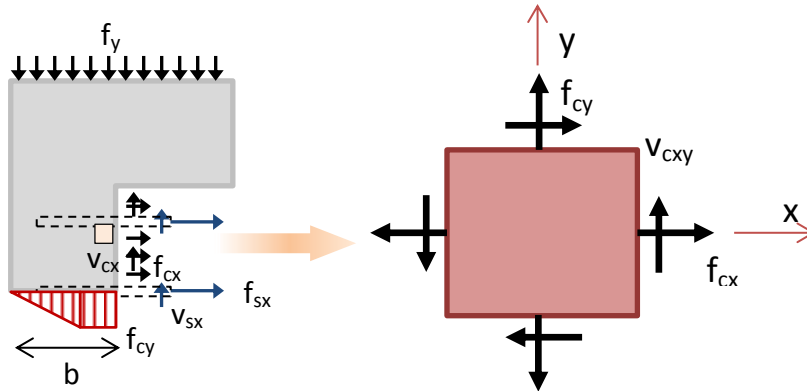

Figure 4. a) Push-off specimen free body diagram, b) Infinitesimal element state of stress

In order to examine the influence of the materials' properties on the behavior of the specimens under direct push off, the problem is analyzed in terms of the stress state, by considering plane-stress transformation on an infinitesimal element of the free body of Fig. 4(a) located at the midheight of the shear plane (Fig. 4(b)). Forces acting on the free-body diagram are shown in Fig. 4 (a) by considering concrete as a new material with its own characteristics acting simultaneously with the reinforcement (Vecchio and Collins 1986). The vertical stresses f_{cy} acting on the bottom side of the cut are assumed to have a triangular distribution being zero on the edge of the specimen, and increasing linearly over 2/3 of the breadth of the resisting

section (2b/3) and the stress is considered constant on the remaining length of b/3. Normal stresses acting on the shear plane are those of the cementitious composite f_{cx} and of the steel reinforcement f_{sx}, while tangential components are v_{cxy} from concrete and v_{sx} from the reinforcement. Equilibrium of forces on the x and y axis is given by Eq. 1 and 2, resulting in the stresses acting on an element of the material at the midheight of the shear plane as shown in Fig. 4 (b).

$$\int_A f_x dA = \int_{A_c} f_{cx} dA_c + \int_{A_s} f_{sx} dA_s = 0 \Rightarrow \int_{A_c} f_{cx} dA_c = -\int_{A_s} f_{sx} dA_s \Rightarrow f_{cx} = -f_{sx} \cdot \rho_{sx} \quad (1)$$

$$\int_A f_y dA = \int_{A_c} v_{cx} dA_c + \int_{A_s} v_{sx} dA_s + \int_B f_{cy} dB \Rightarrow P = v_{cx} \cdot A_c + v_{sx} \cdot A_s + f_{cy} \cdot \frac{2b \cdot d}{3} \quad (2)$$

$$f_{cx} = -f_{sx} \cdot \rho_{sx}, \qquad f_{cy} = -\frac{3P}{4b \cdot d}, \ v_{cxy} = \frac{0.5 \cdot P - 0.5 \cdot v_{sx} \cdot A_s}{0.5 \cdot A_c} = \frac{P - v_{sx} \cdot A_s}{A_c} \quad (3)$$

In the case of the HVFA and SHFRCC specimens with no steel reinforcement crossing the shear plane the stresses f_{cx}, f_{sx} and v_{sx}, are set equal to zero. This results in shear stresses that are equal to the force acting on the specimen divided by the shear plane (b=125 mm, d=100 mm, A_c=20000 mm^2). This value is assumed to correspond to the maximum shear strength of the cementitious material and therefore it is taken to have the same value in the case of the steel reinforced specimens HVFA-S and SHCC-S. With this approach the dowel action of the steel reinforcement is obtained from the difference of load resistance between otherwise identical reinforced and unreinforced specimens. The orientation of the principal normal stresses θ_p (positive value rotates the x axis anticlockwise), the principal stresses σ_1 and σ_2, as well as the principal shear stress $\tau_{cxy,max}$ are calculated as per (Hibbeler 2013):

$$\tan 2\theta_p = v_{cxy} / \left(0.5 \cdot \left(f_{cx} - f_{cy}\right)\right) \quad (6)$$

$$\sigma'_x = 0.5 \cdot \left(f_{cx} + f_{cy}\right) + 0.5 \left(f_{cx} - f_{cy}\right) \cdot \cos 2\theta_p + v_{cxy} \cdot \sin 2\theta_p = \sigma_1 \quad (7)$$

$$\sigma'_y = 0.5 \cdot \left(f_{cx} + f_{cy}\right) - 0.5 \cdot \left(f_{cx} - f_{cy}\right) \cdot \cos 2\theta_p - v_{cxy} \cdot \sin 2\theta_p = \sigma_2 \quad (8)$$

$$\tau_{cxy,max} = \sqrt{v_{cxy}^2 + \left(0.5 \cdot \left(f_{cx} - f_{cy}\right)\right)^2} \quad (9)$$

Figure 5 gives the principal stresses and shear in the case of an element of the HVFA specimen that has no steel reinforcement or fibers in the mix design. While values of the principal tensile stresses are lower than the tensile strength of the material, shear stresses hold values close to its tensile strength (2 MPa). Table 5 gives the stress analysis results for the four different cases examined within this study. The horizontal stress on the cross section f_{cx} in the case of the SHFRCC is an inherent confining stress whose magnitude is equal and opposite to the split cylinder tensile strength as per Georgiou and Pantazopoulou 2017b, while for the case of the

reinforced SHFRCC are equal to the sum of the split tensile strength and the dowel action of the HVFA specimen. The maximum shear stresses τ_{xymax} and the angle of the shear plane θ_s are also listed in Table 4. In the case of the SHCC-S the contribution of the cementitious composite in shear v_{cxy} is considered to be developed due to friction. The friction coefficient may be estimated from the case of the SHFRCC as $\mu=v_{cxy}/f_{cx}=4.67/6.37=0.733$ therefore for the case of SHFRCC-S $v_{cxy}=0.733\cdot8.91=6.54$ MPa.
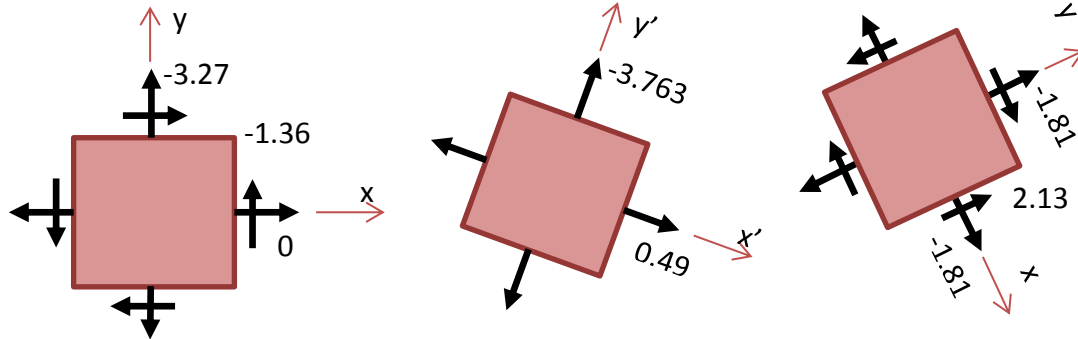

Figure 5. a) Element of HVFA, b) Principal normal stresses, c) maximum shear stresses

Table 4. Stress analysis of all specimens

	HVFA	**HVFA-S**	**SHFRCC**	**SHFRCC-S**
ρ_{sx}	0	0.008482	0	0.008482
f_{sx}	300	300	300	300
f_{cx}	0.00	-2.54	-6.37	-8.91
f_{cy}	-3.27	-9.14	-11.21	-12.72
P_{max}	54.49	152.41	186.82	212.07
v_{sx}	0.00	-8.98	0.00	-17.14
v_{cxy}	-1.36	-1.36	-4.67	-6.54
θ_p	-19.90	-11.22	-31.31	-36.88
$\sigma_{x'}=\sigma_1$	0.49	-2.27	-3.53	-4.01
$\sigma_{y'}=\sigma_2$	-3.76	-9.41	-14.05	-17.63
θ_s	-64.90	-56.22	-76.31	-81.88
$\tau_{x'y'max}$	2.13	3.57	5.26	6.81

CONCLUSIONS

In this paper the combined action of conventional stirrups and fibers was investigated in order to estimate the contribution of fibers to shear strength of SHFRCC. A number of push-off tests were carried out on a new type of sustainable cementitious mix design consisting of 60% of cement replacement with Fly Ash

(Class F), with no coarse aggregate in the mix design and a low water cement content. The shear capacity of this ductile cementitious composite differs from that of normal concrete wherein aggregate interlock is an important contributor to shear strength. The composite was also improved by the use of short discontinuous Polyvinyl Alcohol (PVA) fibers at 2% by volume of the total mix and the results were compared to the mix design without fibers. The results showed a correlation of the push off shear stress to the splitting tensile strength of the cementitious composite materials used for the specimens but not to the direct tensile strength.

REFERENCES

Archontas, N.D., Pantazopoulou, S.J., "Microstructural behavior and mechanics of nano-modified cementitious materials". Adv. Concr. Constr., 3 (2015) 15–37.

ASTM C496: Standard Test Method for Splitting Tensile Strength of Cylindrical Concrete Specimens. ASTM Int. 1–5 (2006).

Buyukozturk, O., Bakhoum, M., Beattie, S., "Shear behavior of joints in precast concrete segmental bridges". J. Struct. Eng., 116 (1990) 3380–3401.

Georgiou, A. V., Pantazopoulou, S.J., "Use of Waste Fly Ash from Power Plants for Use in Cementitious Composites for Structural Elements". In Proceedings of the 4th International Conference on Sustainable Solid Waste Management, Limassol, Cyprus (2016)(a).

Georgiou, A. V., Pantazopoulou, S.J., "Effect of fiber length and surface characteristics on the mechanical properties of cementitious composites". Constr. Build. Mater., 125 (10) (2016)(b) 1216-1228.

Georgiou, A. V., Pantazopoulou, S.J., "Behavior of Strain Hardening Cementitious Composites in Flexure / Shear. J. Mater. Civ. Eng. 29 (2017)(a) 1–15.

Georgiou, A. V., Pantazopoulou, S.J., "Experimental investigation on the confining effect of fibers in SHFRCC". Compos. Struct., (2017)(b).

Georgiou, A. V., Pantazopoulou, S.J., Petrou, M., "Increasing ductility of FRCC with proprietary coating agents". In Proceedings of the 10th fib International PhD Symposium in Civil Engineering., Quebec City, Canada (2014).

Hibbeler, R.C., «Mechanics of Materials», Pearson Prentice Hall (2013).

Li, V.C., Wu, C., Wang, S., Ogawa, A., Saito, T., "Interface Tailoring for Strain-Hardening Polyvinyl Alcohol- Engineered Cementitious Composite (PVA-ECC)". ACI Mater. J., 99 (2003) 463–472.

Naaman, A.E., Reinhardt, H., "Proposed classification of HPFRC composites based on their tensile response". Mater. Struct., 39 (2006) 547–555.

Toshiyuki, K., Kabele, P., Fukuyama, H., Uchida, Y., Suwada, H., Slowik, V., «Strain Hardening Cement Composites: Structural Design and Performance». Springer Netherlands, Dordrecht (2013).

Valle, M., Buyukozturk, O., "Behavior of fiber reinforced high-strength concrete under direct shear". ACI Mater. J., 90, No. 2 (1993) 122–133.

Vecchio, F.J., Collins, M.P., "The modified compression field theory for reinforced concrete elements subjected to shear". ACI Struct. J. 83, No. 2 (1986) 219–231.